Pulling Peptides across Nanochannels: Resolving Peptide Binding and Translocation through the Hetero-oligomeric Channel from *Nocardia farcinica*

Pratik Raj Singh, Iván Bárcena-Uribarri, Niraj Modi, Ulrich Kleinekathöfer, Roland Benz, Mathias Winterhalter,* and Kozhinjampara R Mahendran*

Jacobs University Bremen, Campus Ring 1, D-28759 Bremen, Germany

ABSTRACT We investigated translocation of cationic peptides through nanochannels derived from the Gram-positive bacterium *Nocardia farcinica* at the single-molecule level. The two subunits NfpA and NfpB form a hetero-oligomeric cation selective channel. On the basis of amino acid comparison we performed homology modeling and obtained a channel structurally related to MspA of *Mycobacterium smegmatis*. The quantitative single-molecule measurements provide an insight into transport processes of solutes through nanochannels. High-resolution ion conductance measurements in the presence of peptides of different charge and length revealed the kinetics of peptide binding. The observed asymmetry in peptide binding kinetics indicated a unidirectional channel insertion in the lipid bilayer. In the case of cationic peptides, the external voltage acts as a driving force that promotes the interaction of the peptide with the channel surface. At low voltage, the peptide just binds to the channel, whereas at higher voltage, the force is strong enough to pull the peptide across the channel. This allows distinguishing quantitatively between peptide binding and translocation through the channel.

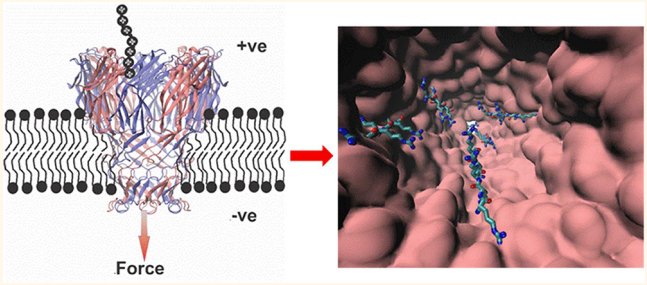

KEYWORDS: *Nocardia* · cationic peptides · applied voltage · binding kinetics · affinity

Bacterial cells continuously need to exchange small molecules, nutrients, and proteins with the exterior environment, simultaneously keeping toxic substances out. Selective transport of molecules through the cell wall is a fundamental process in bacterial life. Many of these processes involve channels made by aggregation of peptides, membrane proteins, or receptors.[1−6] For example, the cell walls of Gram-positive bacteria contain a thick peptidoglycan layer, which allows the permeation of hydrophilic substances up to a molecular mass of 100 kDa.[7] From this follows that unlike Gram-negative bacteria, Gram-positive bacteria do not require pore-forming proteins in their cell wall to transport hydrophilic molecules.[5,7] However, among this group of bacteria, a subgroup belonging to the order actinomycetales contains an even thicker cell wall with a large amount of lipid covalently linked *via* arabinogalactan to the peptidoglycan layer, termed mycolic acid.[7] This thick lipid layer is called the mycolic acid layer because of the presence of long-chain mycolic acids. It represents a second permeability barrier besides the cytoplasmic membrane. In recent years, water-filled pores have been identified in the mycolic acid layer of certain bacteria that allow the permeation of hydrophilic molecules into the space between the inner membrane and the mycolic acid layer. A well-studied channel belonging to this class of membrane channels includes MspA, a major porin of *Mycobacterium smegmatis*, mediating the exchange of hydrophilic solutes across the outer membrane.[7−9]

* Address correspondence to k.mahendran@jacobs-university.de, m.winterhalter@jacobs-university.de.

Received for review August 25, 2012 and accepted November 2, 2012.

Published online November 02, 2012
10.1021/nn303900y

This porin has an octameric goblet-like conformation. The constriction zone of the octameric MspA channel consists of 16 aspartate residues (D90/D91) creating a high density of negative charges, which likely explains the high cation selectivity of this porin.[8] Similar to *M. smegmatis*, the cell wall of the Gram-positive bacterium *Nocardia farcinica* contains also a cation-selective channel composed of two subunits, *N. farcinica porin A* (NfpA) *and N. farcinica porin B* (NfpB), that form together a channel in artificial lipid bilayers.[10−12] The *N. farcinica* channel (NfpA−NfpB) is a hetero-oligomer and structurally related to MspA of *M. smegmatis* based on amino acid comparison. The amino acid sequence alignment suggests an overall amino acid sequence identity of 11% between NfpA, NfpB, and MspA, whereas the identity between NfpA and NfpB is about 52%.[10−12]

The complexity of biological systems makes it important to study specific functions of membrane proteins *in vitro*. Techniques such as electrophysiology, computer simulations, and X-ray crystallography are used to investigate the translocation pathways of antibiotics, nutrients, genetic material (DNA), polyelectrolytes, and peptides across protein channels.[13−19] The purification from the native membrane and reconstitution of the purified protein into an artificial biomimetic membrane is the primary method by which the characterization of membrane proteins can be studied isolated from other components.[20] To obtain initial information on the function of membrane channels, the method of choice is to record the ion currents across the channel.[13,14,17] The underlying measuring principle is the huge difference in ion conductance between the insulating lipid membrane and ion conducting channel, allowing readily a first characterization of single channels with respect to pore size or ion selectivity.[2,16,17,22] Porins reconstituted into liposomes and planar lipid bilayers were recently used for measurements of substrate translocation.[20−22] As the energy barriers for influx of several substrates are asymmetric with channel orientation, it becomes interesting to investigate the orientation of reconstituted porins relative to their directionality *in vivo*.[22,23]

The interaction of polypeptides with transmembrane protein pores is of fundamental importance in biology.[24] Today most studies on the mechanism of protein and peptide translocation across lipid membranes used the ion channels alpha-hemolysin and aerolysin reconstituted into planar lipid bilayers as model translocation systems.[25−31] Here in this work, we express and purify outer membrane porin subunits from *N. farcinica*, NfpA and NfpB, that form hetero-oligomeric channels when reconstituted into planar lipid bilayers. The single-channel properties such as ion conductance, selectivity, and channel gating were investigated. We analyzed also the interaction pathways of the peptides by reconstituting single porins into artificial planar lipid bilayers and measuring the binding of peptides by time-resolved ion current blockages. Homology modeling of the *N. farcinica* channel with respect to MspA indicated that the channel is highly asymmetric in shape, and we probed the orientation of the channel in the lipid bilayers by adding peptides asymmetrically to either the cis or the trans side. Furthermore, we have shown that the entry and exit dynamics of charged peptides of different lengths with respect to the pore can be substantially altered by applying an external electric field. Therefore this effect can change the balance between the forces driving polymers into the pore and the forces driving them out.

RESULTS

Homology Modeling. The structural model of the *N. farcinica* channel was built based upon the Modeler suite of programs.[8,12] Initially, several iterations of the PSI-BLAST protein sequence search program in the PDB database were performed to allow detection of remote homologues of the *N. farcinica* channel. Only the templates with nonredundant structures were kept and further used for building the homology model. These templates included the MspA protein from *M. smegmatis*. The three-dimensional structure of MspA is known (PDB code: 1UUN) and therefore was used as a template to model the *N. farcinica* channel (NfpA−NfpB) structure.[8] From the modeled structure, it can be concluded that the *N. farcinica* channel forms a highly asymmetrically shaped channel similar to MspA, and in its heteroligomeric architecture, two subunits, NfpA and NfpB, are most likely to be arranged in an alternating fashion (Figure 1). In addition, the channel is cation selective with a cluster of negatively charged amino acids distributed through the channel lining and an electrostatic potential surface indicating a highly negative potential inside the lumen of the channel (Figure 1). Moreover, the periplasmic side (stem) of the channel consists of negatively charged residues clustered like a ring, yielding a high charge density, whereas, in the extracellular side (cap), negatively charged residues are scattered rather randomly along the channel surface.

Structural Asymmetry Causes Asymmetric Transport Properties. To test the structural prediction, single *N. farcinica* channels (NfpA and NfpB) were reconstituted into planar lipid bilayers. The single channel conductance was measured to be 3.0 $\pm$ 0.2 nS at 1 M KCl (Figure 2). The channel showed a slight asymmetry of conductance with respect to the polarity of the applied transmembrane potential, supporting the view of an asymmetrical channel reconstituted in lipid bilayers. In addition, the channels showed asymmetric closure with respect to the polarity of the applied voltage. At positive voltages, we observed that the threshold potential for channel closure was around 30 mV, whereas at negative voltage the threshold potential

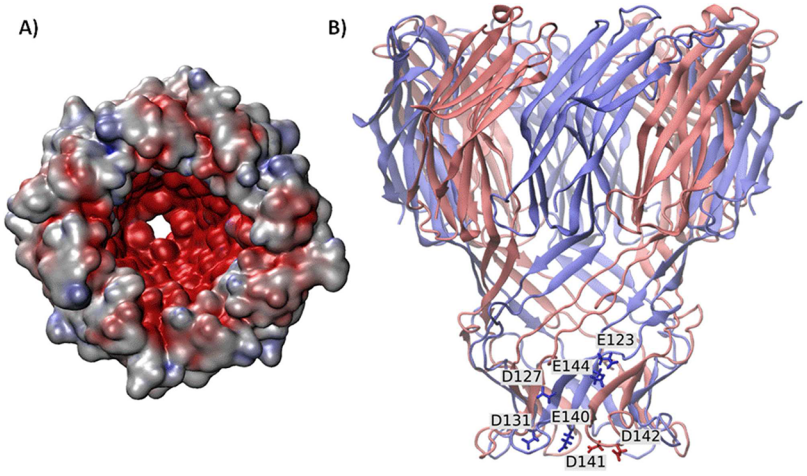

Figure 1. The modeled structure of the *N. farcinica porin A* (NfpA) and *N. farcinica* porin B (NfpB) subunits based on multiple templates of MspA from *M. smegmatis*. Negatively charged amino acid residues are clustered in the channel, resulting in high charge density. (A) Electrostatic potential surface of the modeled structure showing highly negative potential (red color surface) inside the lumen of the channel. (B) Four NfpA and four NfpB subunits are shown in red- and blue-colored secondary structures, respectively, where they are arranged in an alternating fashion. Negatively charged amino acid residues shown as sticks are clustered in the channel stem region, resulting in a high charge density.

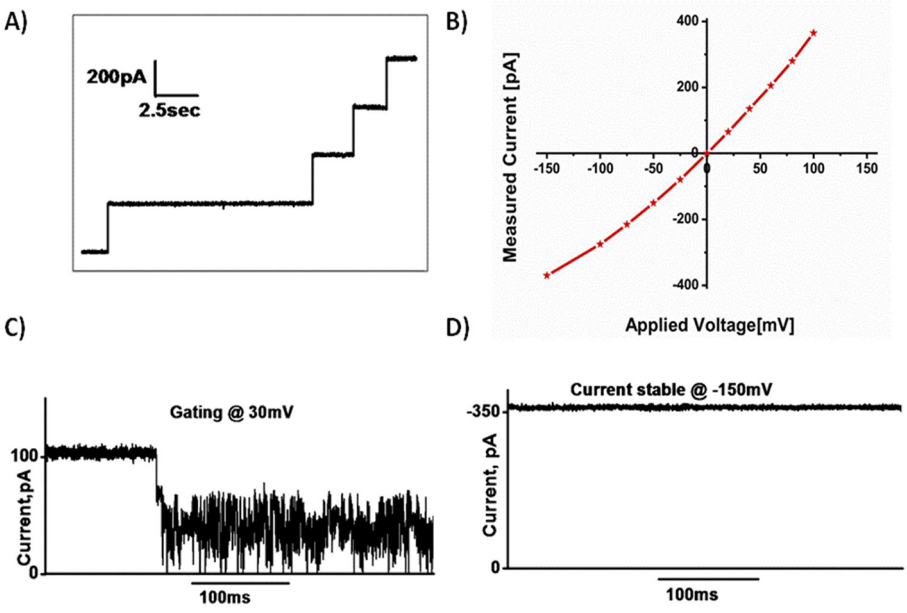

Figure 2. (A) Stepwise insertion of four *N. farcinica* channels reconstituted into planar lipid bilayers at −100 mV. (B) *I*−*V* curve of single-channel *N. farcinica* channel. Ionic currents through single *N. farcinica* channel at (C) +30 and (D) −150 mV. At 30 mV, the channel fluctuates between open and closed conductance state with random gating, whereas at −150 mV the channel exists in one open state. Experimental conditions are 1 M KCl, 10 mM HEPES, pH 7.4.

for channel closure was above 200 mV (Figure 2). The mechanism of this voltage-dependent closure of the channel is so far unclear. Moreover, ion selectivity measurements indicated that the channel is cation selective.[12]

Our model (Figure 1) is used for the interpretation of possible binding sites and their effect on the ion current. To elucidate the effect of the asymmetric structure on the transport properties, we characterized the translocation of differently sized polyarginines (tri, penta, and hepta) using ion current fluctuation analysis. Addition of triarginine to the cis side of the channel hardly induced any ion current blockages, showing negligible interaction of the peptide with the channel surface (Figure 3A). Titrating the channel with penta-arginine caused short, unresolved ion current flickering (Figure 3B). As expected, ion current flickering increased with increasing peptide concentration. Addition of the hepta-arginine causes fluctuations in a concentration- and voltage-dependent manner. However compared to penta-arginine, the number of events is higher (Figure 3C). Under negative potentials

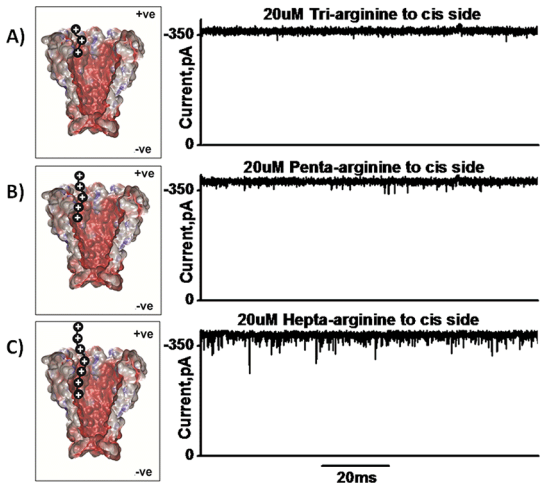

Figure 3. Typical ion current recordings through a single *N. farcinica* channel in the presence of 20 μM (A) triarginine, (B) penta-arginine, and (C) hepta-arginine added to the cis side of the lipid membrane with applied voltage of −150 mV. Experimental conditions are 1 M KCl, 10 mM HEPES, pH 7.4. Corresponding schematic representation showing peptide translocation through the channel driven by applied voltage.

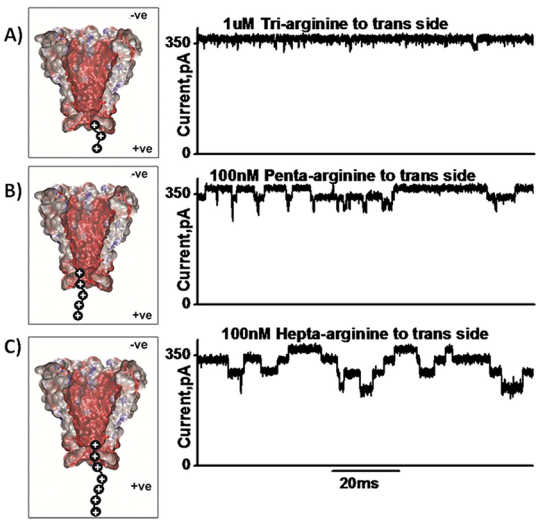

Figure 4. Typical ion current recordings through a single *N. farcinica* channel in the presence of (A) 1 μM triarginine, (B) 100 nM penta-arginine, and (C) 100 nM hepta-arginine added to the trans side of the lipid membrane with applied voltage of +100 mV. Experimental conditions are 1 M KCl, 10 mM HEPES, pH 7.4. Corresponding schematic representation showing peptide translocation through the channel driven by applied voltage.

the addition of peptides on the cis side of the chamber increased the number of events, whereas positive voltages had no effect (*i.e.*, created no blockage events). We hypothesize that when peptide enters the channel through the extracellular side, there is enough space for the ions to pass through, which means cis side addition of the peptide does not produce pronounced blocking.

Reversing the external voltage and the side of peptide addition revealed the asymmetry of the channel. Addition of peptides to the trans side induced pronounced blocking of the channel, indicating strong interaction with the channel surface but with reversed voltage dependence: positive voltages induced ion current blockages, whereas at negative voltages no ion current blockages were produced. As mentioned above, the frequency of channel closure (gating) in the absence of the peptide drastically increased at positive voltages. To distinguish between spontaneous and peptide-induced gating of the channel, we selected the time interval that showed only little intrinsic gating. Triarginine (1 μM) added to the trans side of the membrane produced short but visible ion current blockage events (Figure 4A). In contrast, penta-arginine and hepta-arginine strongly interacted with the channel, resulting in ion current blockages in different steps with reduction in the ion conductance (Figure 4B and C). The corresponding amplitude histogram showing the different conductance states is shown in supplementary Figure 1. This indicated that longer peptides have multiple binding sites in the channel. It is important to note that a concentration in the low nanomolar range of these peptides added to the trans side is strong enough to block the channel as compared to addition of peptide to the cis side. The strength of the channel−peptide interaction is in the order hepta-arginine > penta-arginine > triarginine. The channel blockades caused by the peptides penta-arginine and hepta-arginine are greater in amplitude and duration than those for a short peptide, triarginine. We hypothesize that in the case of trans side addition of the peptide, the negative charges clustered in rings on the periplasmic entry strongly interact with the peptide and there is only limited space for the ions to pass through. As a result, we observed strong blocking of the channel by the peptide. From the asymmetrical addition of the peptide, we concluded that the channel is oriented in the bilayers with the extracellular part at the cis side and the periplasmic part inserted into lipid bilayers that can easily be accessed from the trans side.

Previously it has been shown that noise analysis of the single-channel level revealed asymmetries in channel transport.[14,22] Such asymmetries are often hidden in membrane preparations with multiple insertions, in which the channel orientation appeared to be equally distributed. Previous analysis of the ion current fluctuations under asymmetric conditions revealed that the kinetics of sugar entry depends on the side of addition for maltoporin reconstituted into artificial lipid bilayers.[22] Moreover, chemical modifications of the sugar allowed only the entry of the sugar on one side but no permeation. This enabled us to distinguish translocation from entry and bouncing back to the same side. It has been shown that maltoporin catalyzes the transport more efficiently from the outside to the inside than under reversed asymmetric conditions.[14,22,23,34]

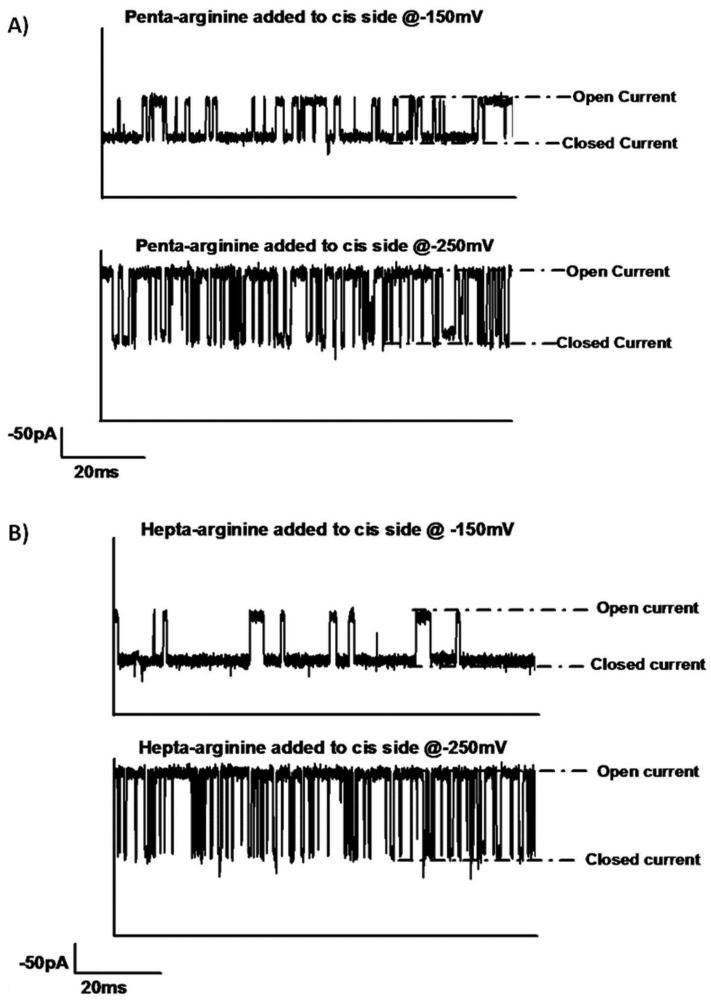

Figure 5. Typical ion current recordings through a single *N. farcinica* channel in the presence of (A) penta-arginine added to the cis side at −150 and −250 mV and (B) hepta-arginine added to the *cis* side at −150 and −250 mV. The closed current represents the time spent by the peptide in the channel or the residence time of the peptide. Experimental conditions are 150 mM KCl, 10 mM HEPES, pH 7.4.

Here we extended our study toward interaction of peptides with the hetero-oligomeric channel from *N. farcinica*. As shown in Figure 1, the channel consists of an extracellular part of large diameter, whereas the periplasmic side consists of a rather narrow opening. The addition of cationic peptides of different charge and length produced an asymmetry in the peptide binding kinetics that can be used to distinguish the orientation of the channel reconstituted into lipid bilayers.

Resolving Binding and Translocation. To elucidate the electrostatic contributions of peptide interaction with the channel surface, we reduced the salt concentration from 1 M to 150 mM KCl and investigated the peptide binding kinetics by single-channel analysis. Addition of penta-arginine and hepta-arginine to the cis side of the channel produced well-defined ion current blockage events. The channel fluctuated between the fully open conductance state and the closed conductance state (Figure 5). The frequency and duration of the ion current fluctuations depended strongly on the applied voltage and peptide concentration. The number of peptide blocking events and the average residence time of the peptide blockage increased at low salt concentration, which indicated charge effects on the peptide−channel interaction. The peptide binding kinetics was derived from the two factors τ_c (blockage time) and τ_o (open time or time between successful blockage) fitted with an exponential fit of the open and closed time histogram. We found that the reciprocal of τ_o (the mean interevent interval) is linearly dependent on the polypeptide concentration, whereas τ_c (the mean dwell time) is independent of the polypeptide concentration. The applied voltage serves as the main driving force to pull the cationic peptides from the aqueous bath to the channel surface. We plotted τ_c and τ_o as a function of the applied voltage from −100 mV to −250 mV for the cis side addition of the peptide (Figure 6). The plot of average residence time as a function of the applied voltage allows distinguishing peptide binding from the translocation. The τ_c is higher for hepta-arginine as compared to penta-arginine (supplementary

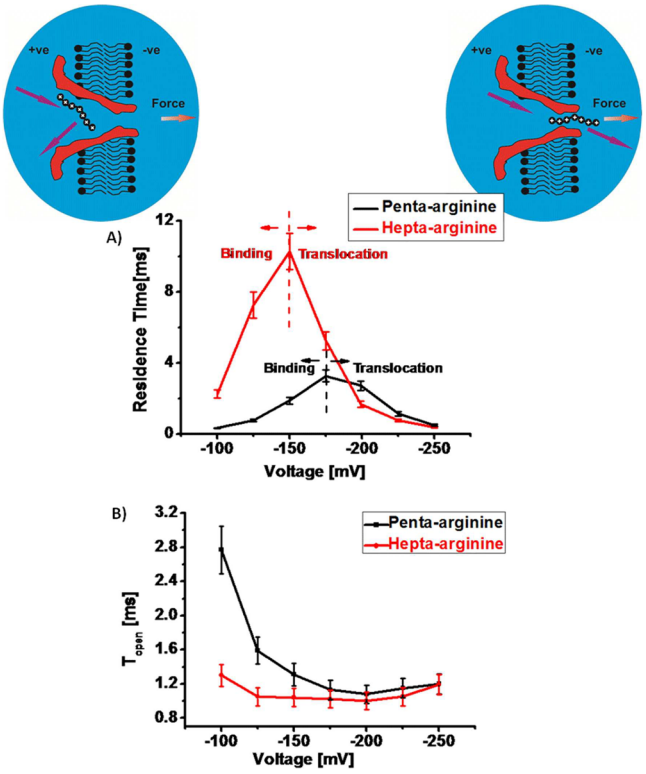

Figure 6. (A) The residence time and (B) the open channel time as a function of the applied voltage (−100 to −250 mV) for penta-arginine and hepta-arginine. Experimental conditions are 150 mM KCl, 10 mM HEPES, pH 7.4. Peptide is added to the cis side of the channel.

TABLE 1. Rate Constants of Peptide Association (k_{on}) and Dissociation (k_{off}) and Equilibrium Binding Constant K of the Interaction between Peptide and *Nocardia farcinica* Channel

penta-arginine				hepta-arginine			
voltage [mV]	K_{on} [M^{-1} s^{-1}] × 10^9	K_{off} [s^{-1}] × 10^3	K [M^{-1}] × 10^7	voltage [mV]	K_{on} [M^{-1} s^{-1}] × 10^9	K_{off} [s^{-1}] × 10^3	K [M^{-1}] × 10^7
−100	2.5 ± 0.2	2.4 ± 0.24	0.11 ± 0.01	−100	7.7 ± 0.8	0.4 ± 0.04	1.74 ± 0.02
−150	5.8 ± 0.5	0.6 ± 0.05	1.06 ± 0.1	−150	9.6 ± 0.9	0.09 ± 0.01	9.88 ± 0.04
−250	7.6 ± 0.7	1.9 ± 0.20	0.39 ± 0.04	−250	8.4 ± 0.8	2.7 ± 0.3	0.31 ± 0.02

Figure 2). In case of hepta-arginine τ_c increased with increasing voltage from −100 mV to −150 mV, which indicated that hepta-arginine just binds to the channel without effective translocation. Surprisingly, when the voltage was increased above −150 mV, we observed a decrease in the average residence time with increasing voltage, suggesting successful translocation of the peptide through the channel. The threshold potential for pulling hepta-arginine through the channel was calculated to be ∼−150 mV, where force is strong enough to drag the peptide from the binding site of the channel. In the case of penta-arginine, we observed a similar behavior of increase in the residence time at lower voltages and a decrease in residence time at higher voltage. However, the threshold potential for effective translocation to pull the peptide out of the channel was calculated to be ∼−175 mV. The τ_o decreased with increasing concentration of peptide and increasing applied voltage. Addition of the peptide to the trans side completely closed the channel due to strong binding at low salt concentration caused by charge effects. Subsequently τ_o and τ_c could not be obtained. The results suggested a simple bimolecular interaction between the polypeptide and the pore. The rate constants of association k_{on} can be derived from the slopes of plots of $1/\tau_o$ *vs* [pept], where [pept] is the peptide concentration in the aqueous phase. The rate constants of dissociation (k_{off}) were determined by averaging the $1/\tau_c$ values recorded over the whole concentration range. The equilibrium association constant was then calculated by using $K = k_{on}/k_{off}$, which gives the affinity of the peptide to the channel. Peptide binding kinetics for penta-arginine and hepta-arginine are summarized in Table 1.

Most approaches investigate the modulation of the ion current through channels in the presence of permeating solutes caused by slight size differences.[13,17,33] However, the translocation of macromolecules through nanopores is not only determined by the size but to a large extent also influenced by electrostatic,

hydrodynamic, hydrophobic, and van der Waals interactions with the nanopore walls.[13−19] The quantification of transported uncharged molecules across a few nanometer long channels remains experimentally a challenge. Ensemble measurements on liposomes (liposome swelling) have only a limited time resolution.[20] The above-described method of noise analysis of the ion current has a number of unique advantages, among others, the use of very little material with single-molecule resolution, the potential for parallelization, and the relatively good time resolution. However, with respect to the translocation of uncharged molecules, a direct conclusion from binding on transport is not possible.[32] In contrast for charged compounds, the applied transmembrane voltage is the driving force to pull the molecule out of the channel.

In particular pulling DNA through nanopores for next-generation sequencing remains a very prominent research area.[6,19,36] Despite the rapid development of single-molecule techniques, the underlying mechanisms and forces in this molecular transport are poorly characterized and not fully understood. Previously it has been shown that solid-state nanopores and biological nanopores have been used to study the coupling between protein translocation and folding.[7,24,28−31,33] This allows for detection and analysis in real-time protein translocation events. For example, alpha hemolysin was used to study the partitioning of synthetic cationic alanine-based peptides.[25−27] The kinetics of association and dissociation rate constants obtained from a single alpha hemolysin channel in the presence of micromolar concentrations of peptide are strongly dependent on the transmembrane voltage and peptide length.[31]

CONCLUSION

Here in this work, we introduced a new type of channel, a novel hetero-oligomeric nanochannel derived from *N. farcinica*. In the present contribution, we showed an experimental strategy to illuminate various kinetic contributions to polypeptide translocation through the *N. farcinica* channel reconstituted into lipid bilayers. We have been able to measure time-resolved single-molecule events of peptide entry into the pore and obtain detailed kinetic information. Moreover, it has been discussed that *N. farcinica* channels reconstituted into planar lipid bilayers have asymmetric properties in both ion conductance and peptide binding. This asymmetry in the peptide binding reveals that channel insertion is unidirectional. The applied transmembrane voltage acts as a possible driving force for diffusion of cationic macromolecules through the channel. We hypothesize that the binding is enhanced at low voltages and that with increasing applied voltage the peptide is pulled out of the channel, resulting in successful translocation. The kinetic data obtained from our single-channel measurements can be used to distinguish the peptide binding events from the translocation events. In conclusion this work demonstrates that a biological nanopore can represent a versatile single-molecule tool for exploring protein interactions.

METHOD

Purification of Two Subunits of Porins from *Nocardia farcinica*. The purification of the two subunits NfpA and NfpB expressed in *E. coli* BL21 (DE3) Omp8 was performed as described previously.[12,37] In brief, the genes flanked with 10 histidine residues were cloned into the expression plasmid pARAJS2 containing an arabinose-induced promoter sequence.[38] This plasmid had been prepared, and the porin-deficient *E.coli* Omp8 cells containing the plasmid were grown in an LB-ampicillin media at 37 °C until it reached the OD_{600} of 0.5−0.9. The cells were then induced with 0.02% of arabinose for overexpression and were grown at 16 °C for 16 h. The cell broth was centrifuged at 5000*g* for 10 min at 4 °C, and the pellet was resuspended in 10 mM Tris pH 8. The resuspended pellet was later broken down by French press, and the cell debris was obtained by centrifugation at 5000*g* for 10 min at 4 °C. The supernatant was ultracentrifuged at 48000*g* for 1 h at 4 °C to obtain a supernatant containing the cytosolic proteins and the pellet containing membrane proteins. Our proteins of interest were found to be present in both the supernatant and pellet fractions. The protein present in the supernatant fraction was obtained as inclusion bodies that were not large enough to pellet down during ultracentrifugation. The temperature of 16 °C used for cell growth after induction with arabinose facilitated the smaller aggregation of proteins as inclusion bodies. Nevertheless, the His-Tag protein purification from the supernatant fraction had to be performed under denaturating conditions using urea buffer. The purification under denaturating conditions was performed by suspending 1 mL of the supernatant in 4 mL of 8 M urea/10 mM Tris/200 μL Ni-Sepharose High Performance/20 mM imidazole pH 8 buffer for 6 h at room temperature. The beads were then extensively washed with 8 M urea/10 mM Tris/100 mM imidazole pH 8 to remove impurities. Later the NfpA/NfpB proteins were eluted with the solution containing 8 M urea/10 mM Tris/500 mM imidazole pH 8. The expression and purification of proteins were monitored by SDS page and Western blot in every step. The two subunits, purified separately, were refolded together to form a hetero-oligomeric channel by ammonium sulfate precipitation. The two purified subunits were mixed together in a 1:1 ratio and precipitated using saturated ammonium sulfate solution. The solution was incubated overnight and was centrifuged at 18000*g* for 30 min to remove the supernatant. The precipitated protein pellet was refolded to native state by incubating for 12 h in 10 mM Tris-HCl with 1% Triton X-100 and 150 mM NaCl.[12]

Solvent-Free Lipid Bilayer Technique. Reconstitution experiments and noise analysis have been performed as described in detail previously.[32,35] The phospholipid bilayer was formed with DPhPC (1,2-diphytanoyl-*sn*-glycero-3-phosphocholine) by employing the classic Montal and Muller technique.[35] A Teflon cell with an approximately 50 μm diameter aperture in the 25 μm thick Teflon partition was placed between the two chambers of the cuvette. The aperture was small enough to form a stable bilayer with the possibility of protein insertion. As the electrolyte, 1 M KCl, 10 mM HEPES, pH 7.4 was used and added to both sides of the chamber unless otherwise indicated. Standard silver−silver chloride electrodes from WPI (World Precision Instruments) were placed in each chamber to measure the ion current. For single-channel measurement, small amounts of porin were added to the cis-side of the chamber

(side connected to the ground electrode). Spontaneous channel insertion was usually obtained while stirring under applied voltage. In order to prevent insertion of more than one porin, the cis side of the chamber was carefully diluted with the same buffer to remove the remaining channels. Conductance measurements were performed using an Axopatch 200B amplifier (Axon Instruments) in the voltage clamp mode. Signals were filtered by an on board low pass Bessel filter at 10 kHz and recorded onto a computer hard drive with a sampling frequency of 50 kHz. Amplitude, probability, and noise analyses were performed using Origin (Microcal Software Inc.) and Clampfit (Axon Instruments) software. Single channel analysis was used to determine the peptide binding kinetics. To obtain good statistics for the results, the experiments were repeated five times with different *N. farcinica* channels. We determined the association and dissociation rate constants and the partitioning data from single-channel recordings of the *N. farcinica* channel. In a single-channel measurement the usual measured quantities as illustrated in Figure 6 are the duration of closed levels residence time (τ_c) and open channel time (τ_o), or for short blockages the average residence time (τ_c) and the number of blockage events per second.

Conflict of Interest: The authors declare no competing financial interest.

Acknowledgment. The authors are grateful for financial support through the Deutsche Forschungsgemeinschaft (DFG WI 2278/18-1) and from Jacobs University Bremen.

Supporting Information Available: Amplitude histogram showing fluctuation of the channel between different conductance steps in the presence of penta-arginine and hepta-arginine; dwell time histogram for closed time and open time in the presence of penta-arginine and hepta-arginine; concentration dependence of peptide interaction with the channel; hepta-arginine added to trans side of the chamber at low salt concentration. This information is available free of charge *via* the Internet at http://pubs.acs.org.

REFERENCES AND NOTES

1. Benz, R.; Janko, K.; Boos, W.; Läuger, P. Formation of Large, Ion-Permeable Membrane Channels by the Matrix Protein (porin) of *Escherichia coli*. *Biochim. Biophys. Acta* **1978**, *511*, 305–319.
2. Mueller, P.; Rudin, D. O. Induced Excitability in Reconstituted Cell Membrane Structure. *J. Theor. Biol.* **1963**, *4*, 268–280.
3. Benz, R.; Schmid, A.; Hancock, R. E. Ion Selectivity of Gram-Negative Bacterial Porins. *J. Bacteriol.* **1985**, *162*, 722–727.
4. Luckey, M.; Nikaido, H. Diffusion of Solutes Through Channels Produced by Phage Lambda Receptor Protein of *Escherichia coli*: Inhibition by Higher Oligosaccharides of Maltose Series. *Biochem. Biophys. Res. Commun.* **1980**, *93*, 166–171.
5. Nikaido, H. Porins and Specific Channels of Bacterial Outer Membranes. *Mol. Microbiol.* **1992**, *6*, 435–442.
6. Hall, A. R.; Scott, A.; Rotem, D.; Mehta, K. K.; Bayley, H.; Dekker, C. Hybrid Pore Formation by Directed Insertion of Alpha-Hemolysin into Solid-State Nanopores. *Nat. Nanotechnol.* **2011**, *5*, 874–877.
7. Brennan, P. J.; Nikaido, H. The Envelope of Mycobacteria. *Annu. Rev. Biochem.* **1995**, *64*, 29–63.
8. Faller, M.; Niederweis, M.; Schulz, G. E. The structure of a Mycobacterial Outer-Membrane Channel. *Science* **2004**, *303*, 1189–1192.
9. Stahl, C.; Kubetzko, S.; Kaps, I.; Seeber, S.; Engelhardt, H; Niederweis, M. MspA Provides the Main Hydrophilic Pathway through the Cell Wall of *Mycobacterium smegmatis*. *Mol. Microbiol.* **2001**, *40*, 451–464.
10. Riess, F. G.; Lichtinger, T.; Yassin, A. F.; Schaal, K. P.; Benz, R. The Cell Wall Porin of The Gram-Positive Bacterium *Nocardia asteroides* forms Cation-Selective Channels that Exhibit Asymmetric Voltage Dependence. *Arch. Microbiol.* **1999**, *171*, 173–182.
11. Riess, F. G.; Lichtinger, T.; Cseh, R.; Yassin, A. F.; Schaal, K. P.; Benz, R. The Cell Wall Porin of *Nocardia farcinica*: Biochemical Identification of The Channel-Forming Protein and Biophysical Characterization of The Channel Properties. *Mol. Microbiol.* **1998**, *29*, 139–150.
12. Kläckta, C.; Knörzer, P.; Riess, F.; Benz, R. Hetero-Oligomeric Cell Wall Channels (porins) of *Nocardia farcinica*. *Biochim. Biophys. Acta, Biomembr.* **2011**, *1808*, 1601–1610.
13. Bezrukov, S. M.; Vodyanoy, I.; Parsegian, V. A. Counting Polymers Moving Through a Single Ion Channel. *Nature* **1994**, *370*, 279–281.
14. Nekolla, S.; Andersen, C.; Benz, R. Noise Analysis of Ion Current Through The Open and The Sugar-Induced Closed State of the LamB Channel of *Escherichia coli* Outer Membrane: Evaluation of the Sugar Binding Kinetics to the Channel Interior. *Biophys. J.* **1994**, *66*, 1388–1397.
15. Aksimentiev, A.; Schulten, K. Imaging Alpha-Hemolysin with Molecular Dynamics: Ionic Conductance, Osmotic Permeability, and the Electrostatic Potential Map. *Biophys. J.* **2005**, *88*, 3745–3761.
16. Merzlyak, P. G.; Yuldasheva, L. N.; Rodrigues, C. G.; Carneiro, C. M.; Krasilnikov, O. V.; Bezrukov, S. M. Polymeric Nonelectrolytes to Probe Pore Geometry: Application to the Alpha-Toxin Transmembrane Channel. *Biophys. J.* **1999**, *77*, 3023–3033.
17. Bezrukov, S. M. Ion Channels as Molecular Coulter Counters to Probe Metabolite Transport. *J. Membr. Biol.* **2000**, *174*, 1–13.
18. Wong, C. T.; Muthukumar, M. Polymer Translocation through Alpha-Hemolysin Pore with Tunable Polymers-Pore Electrostatic Interactions. *J. Chem. Phys.* **2010**, *133*, 045101.
19. Muthukumar, M. Mechanism of DNA Transport through Pores. *Annu. Rev. Biophys. Biomol. Struct.* **2007**, *36*, 435–450.
20. Nikaido, H.; Rosenberg, E. Y. Porin Channels in *Escherichia coli*: Studies with Liposomes Reconstituted from Purified Proteins. *J. Bacteriol.* **1983**, *153*, 241–252.
21. Eren, E.; Vijayaraghavan, J.; Liu, J.; Cheneke, B. R.; Touw, D. S.; Lepore, B. W.; Indic, M.; Movileanu, L.; Van den Berg, B. Substrate Specificity within a Family of Outer Membrane Carboxylate Channels. *PLoS Biol.* **2012**, *10*, e1001242.
22. Danelon, C.; Brando, T.; Winterhalter, M. Probing the Orientation of Reconstituted Maltoporin Channels at the Single-Protein Level. *J. Biol. Chem.* **2003**, *278*, 35542–35551.
23. Kullman, L.; Gurnev, P. A.; Winterhalter, M.; Bezrukov, S. M. Functional Subconformations in Protein Folding: Evidence from Single-Channel Experiments. *Phys. Rev. Lett.* **2006**, *96*, 038101.
24. Dobson, C. M. Protein Folding and Misfolding. *Nature* **2003**, *426*, 884–890.
25. Mohammad, M. M.; Movileanu, L. Excursion of a Single Polypeptide into a Protein Pore: Simple Physics, but Complicated Biology. *Eur. Biophys. J.* **2008**, *37*, 913–925.
26. Movileanu, L.; Schmittschmitt, J. P.; Scholtz, J. M.; Bayley, H. Interactions of Peptides with a Protein Pore. *Biophys. J.* **2005**, *89*, 1030–1045.
27. Wolfe, A. J.; Mohammad, M. M.; Cheley, S.; Bayley, H.; Movileanu, L. Catalyzing The Translocation of Polypeptides through Attractive Interactions. *J. Am. Chem. Soc.* **2007**, *129*, 14034–14041.
28. Oukhaled, G.; Mathé, J.; Biance, A. L.; Bacari, L.; Betton, J. M.; Lairez, D.; Pelta, J.; Auvray, L. Unfolding of Proteins and Long Transient Conformations Detected by Single Nanopore Recording. *Phys. Rev. Lett.* **2007**, *98*, 158101–158104.
29. Pastoriza-Gallego, M.; Rabah, L.; Gibrat, G.; Thiebot, B.; Van der Goot, F. G.; Auvray, L.; Betton, J. M.; Pelta, J. Dynamics of Unfolded Protein Transport through an Aerolysin Pore. *J. Am. Chem. Soc.* **2010**, *133*, 2923–2931.
30. Bikwemu, R.; Wolfe, A. J.; Xing, X.; Movileanu, L. Facilitated Translocation of Polypeptides through a Single Nanopore. *J. Phys.: Condens. Matter* **2010**, *22*, 454117.
31. Meng, H.; Detillieux, D.; Baran, C.; Krasniqi, B.; Christensen, C.; Madampage, C.; Stefureac, R. I.; Lee, J. S. Nanopore Analysis of Tethered Peptides. *J. Pept. Sci.* **2010**, *16*, 701–708.

32. Mahendran, K.; Hajjar, E.; Mach, T.; Lovelle, M.; Sousa, I.; Kumar, A.; Spiga, E.; Weingart, H.; Gameiro, P.; Winterhalter, M.; *et al*. Molecular Basis of Enrofloxacin Translocation through a Bacterial Porin —When Binding does not Imply Translocation. *J. Phys. Chem. B* **2010**, *114*, 5170–5179.
33. Cressiot, B.; Oukhaled, A.; Patriarche, G.; Pastoriza-Gallego, M.; Betton, J. M.; Auvray, L.; Muthukumar, M.; Bacri, L.; Pelta, J. Protein Transport through a Narrow Solid-State Nanopore at High Voltage: Experiments and Theory. *ACS Nano* **2012**, *6*, 6236–6243.
34. Berezhkovskii, A. M.; Bezrukov, S. M. Optimizing Transport of Metabolites through Large Channels: Molecular Sieves with and without Binding. *Biophys. J.* **2005**, *88*, L17–L19.
35. Montal, M.; Müller, P. Formation of Bimolecular Membranes from Lipid Monolayers and a Study of their Electrical Properties. *Proc. Natl. Acad. Sci. U. S. A.* **1972**, *69*, 3561–3566.
36. Wallace, E. V.; Stoddart, D.; Heron, A. J.; Mikhailova, E.; Maglia, G.; Donohoe, T. J.; Bayley, H. Identification of Epigenetic DNA Modifications with a Protein Nanopore. *Chem. Commun. (Cambridge, U.K.)* **2010**, *46*, 8195–8197.
37. Prilipov, A.; Phale, P. S.; Van Gelder, P.; Rosenbusch, J.; Koebnik, R. Coupling Site-Directed Mutagenesis with High-Level Expression: Large Scale Production of Mutant Porins from *E. coli*. *FEMS Microbiol. Lett.* **1998**, *163*, 65–72.
38. Polleichtner, G.; Andersen, C. The Channel-Tunnel HI1462 of *Haemophilus influenzae* reveals Differences to *Escherichia coli* TolC. *Microbiology* **2006**, *152*, 1639–1647.